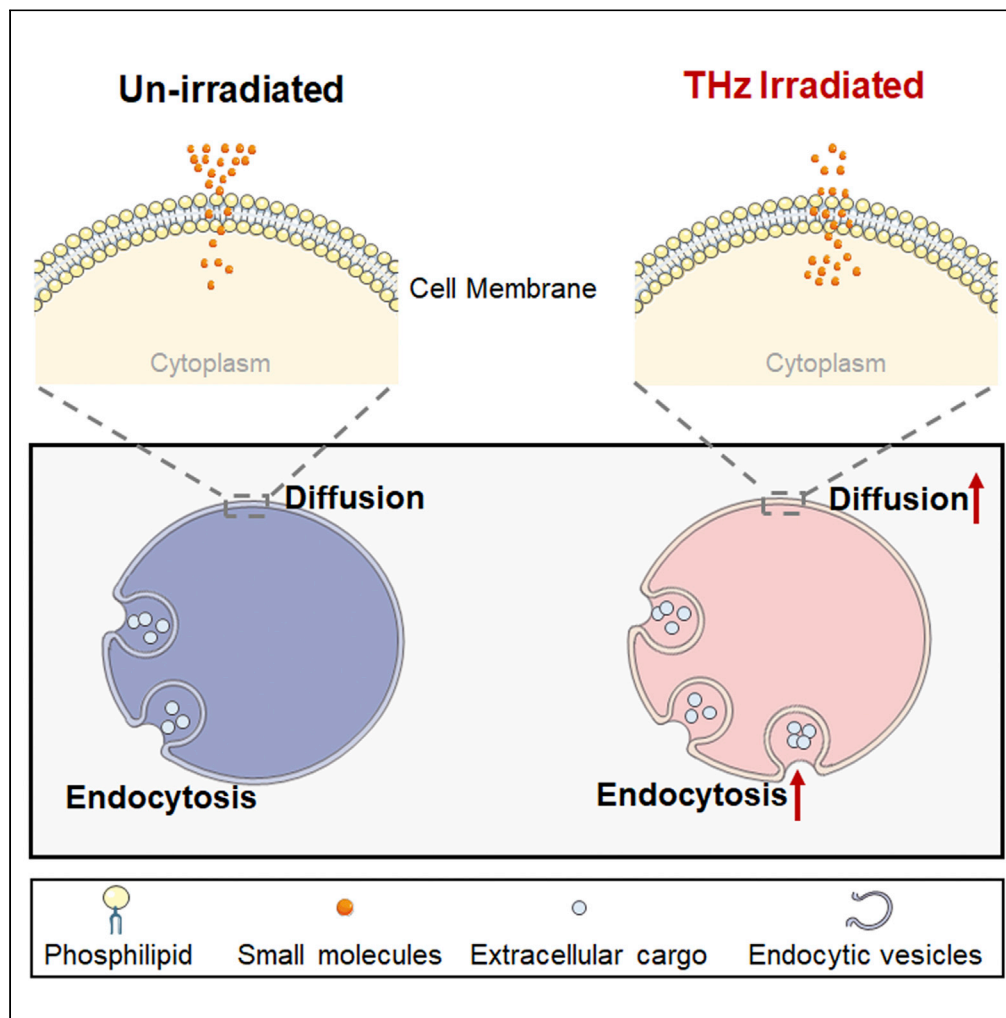


Article

Continuous wave irradiation at 0.1 terahertz facilitates transmembrane transport of small molecules



Erling Hu, Qi Zhang, Sen Shang, Yinan Jiang, Xiaoyun Lu

luxy05@xjtu.edu.cn

Highlights
THz irradiation enhances endocytic activity of neuronal cells

THz irradiation increases the permeation of rhodamine derivatives into cells

THz irradiation promotes the cellular uptake of small drugs GDC0941 and H89

Hu et al., iScience 25, 103966
March 18, 2022 © 2022 The Authors.
<https://doi.org/10.1016/j.isci.2022.103966>



Article

Continuous wave irradiation at 0.1 terahertz facilitates transmembrane transport of small molecules

Erling Hu,¹ Qi Zhang,¹ Sen Shang,¹ Yinan Jiang,¹ and Xiaoyun Lu^{1,2,*}

SUMMARY

The bioeffects of terahertz (THz) radiation received growing attention because of its influence on the interactions between biomolecules. Our work aimed to investigate the effects of THz irradiation on cell membrane, especially cell membrane permeability. We found that 0.1 THz irradiation promoted the endocytosis of FM4-64-labeled cells and the inhibition of dynamin attenuated but did not fully abolish the THz promoted endocytosis. Moreover, 0.1 THz irradiation also promoted the transmembrane of the rhodamine, as well as the chemical compounds GDC0941 and H89, evidenced by the confocal microscope observation and the western blotting analysis, respectively. These findings demonstrated 0.1 THz irradiation facilitated the transmembrane transport of small molecules by promoting both the cellular endocytosis and the diffusion process. Our study provided direct evidence that THz could affect the cell membrane permeability, broadened the THz affected cellular physiological processes, and implied its potential application in regulating the cell membrane functions.

INTRODUCTION

In recent years, terahertz (THz) wave irradiation which is typically defined as the electromagnetic spectrum frequencies ranging from 0.1 to 10 THz has attracted keen interest because of its increased applications in various fields, such as communications, security checks, imaging, and biomedicine (Borovkova et al., 2018; Cheng et al., 2020; Elayan et al., 2018; Ghann et al., 2019). It was shown that certain vibration modes and complex intramolecular interactions of macromolecules including proteins, DNA, RNA, lipids, and polysaccharides can resonate with terahertz waves (Romanenko et al., 2017). Therefore, as a kind of nonionizing radiation, THz radiation is considered to be able to exert potential effects on the biological system in addition to being a good detection tool for biomolecular recognition. It was previously reported that THz radiation does not induce direct damage to biological tissues but did change a variety of biological processes such as inhibiting cell proliferation, changing the adhesive properties of nerve cells, affecting DNA unwinding and gene expression, and inducing apoptosis (Abufadda et al., 2021; Alexandrov et al., 2011; Tang et al., 2020; Williams et al., 2013). Although the biophysical mechanisms underlying these responses are still poorly understood, it is still interesting to figure out some novel bioeffects of THz radiation.

The plasma membrane, which consists mainly of a lipid bilayer approximately 5 nm in width and proteins embedded in the membrane, normally provides a fundamental barrier to most molecular transport in and out of cells. It is essential to control the permeability of the cell membrane for many biotechnological and medical applications because outside cargoes, such as various fluorescent dyes and protein inhibitors which are widely used in various biological assays (Baryawno et al., 2010; Cho et al., 2009; Specht et al., 2017), must first traverse the plasma membrane to reach the intracellular targets. Similarly, many small molecule drugs that target intracellular proteins must cross the plasma membrane to exert their clinical effect (Chen et al., 2019). Moreover, because various signaling proteins are embedded in the plasma membrane, changing the membrane properties or functions may also affect a series of related intracellular signal transduction pathways and cellular functions. It was reported that high frequency THz radiation induced transient cell membrane permeabilization and promoted nanoparticle uptake by PC12 cells (Pera et al., 2019). We also found that 3.1 THz pulsed radiation enhanced the endocytosis of HT22 cells (under submission). Here, we proceeded in investigating the potential effects of low frequency THz continuous waves on the endocytic activity as well as the permeability of the cell membrane in neuronal cells.

¹Key Laboratory of Biomedical Information Engineering of the Ministry of Education, School of Life Science and Technology, Xi'an Jiaotong University, Xi'an 710049, Shaanxi, China

²Lead contact

*Correspondence: luxy05@xjtu.edu.cn

<https://doi.org/10.1016/j.isci.2022.103966>



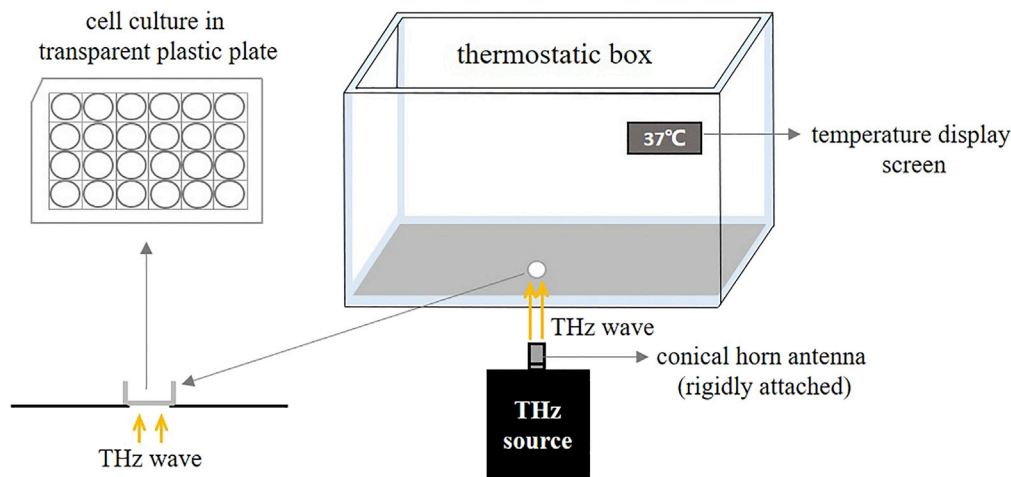


Figure 1. Experimental setup of THz exposure

THz radiation was emitted and directly reached the irradiated samples in an incubator at 37°C. Cells were cultured in a transparent plastic plate and were exposed to the radiation in the period of experiments.

In this study, the murine hippocampal neuronal cell line HT22 was irradiated with 0.1 THz continuous waves, the process of endocytosis, and the diffusion of small molecules was analyzed to investigate the effects of low frequency THz radiation on cell membrane. We found that the 0.1 THz radiation promoted both dynamin-dependent and the dynamin-independent endocytosis of HT22 cells indicated by FM4-64 fluorescent labeling technique. Moreover, 0.1 THz radiation also facilitated the transmembrane diffusion of small molecules into the cells evidenced by both fluorescence and biochemical results. Thus, we uncovered a novel effect of THz waves on the cell membrane functions of neuronal cells, revealing that low frequency THz continuous waves facilitated the transmembrane transport of small molecules via promoting the endocytosis and the diffusion process. It highlights the potential applications of THz in regulating the cell membrane permeability and functions, which is essential for cellular materials and information exchange.

RESULTS

0.1 THz radiation promoted endocytosis in neurons

To assess the influence of the continuous wave irradiation at 0.1 THz on endocytosis in HT22 cells, we used FM4-64, a membrane-selective amphiphilic fluorescent dye that is used routinely to monitor the endocytic process in living eukaryotic cells, to assess the endocytic activity of cells. As shown in Figure 1, the output THz wave was transported to a conical horn antenna rigidly attached at the bottom surface of the transparent plastic cell culture dish to irradiate the samples. The cells were exposed to 0.1 THz radiation under an average power density of 33 mW/cm². The temperature of the mediums in irradiated or nonirradiated cell culture holes was measured by a handheld thermometer and there was no significant difference between the treated group and the untreated group along with the exposure (Figure S1). Cells were imaged by laser confocal microscopy after washing off the excess dye. The laser confocal microscopy observation results demonstrated that higher FM4-64 fluorescence signal was obtained in THz-irradiated cells, and quantitative image analysis also indicated that the average fluorescence intensity of individual cells in the irradiated group was around 50% higher than in the unirradiated group, indicating that the endocytosis was promoted by 0.1 THz radiation treatment (Figure 2). To further determine whether the influence of 0.1 THz radiation is specific to HT22 cells, we performed the same experiment with the pheochromocytoma cell line PC12. Consistently, THz radiation also triggered an increase of the red FM4-64 fluorescence signal in PC12 cells (Figure S2). These results showed that 0.1 THz continuous wave irradiation promoted the cellular endocytic process.

The dynamin-dependent endocytosis is arguably the major endocytic pathway (Ferguson and De Camilli, 2012). Therefore, we used a dynamin inhibitor, Dynasore (N'-(3,4-dihydroxybenzylidene)-3-hydroxy-2-naphthohydrazide) to pretreated the cells to see whether the inhibition of dynamin could totally block the THz induced enhancement of endocytosis. As expected, the internalization of FM4-64 was significantly

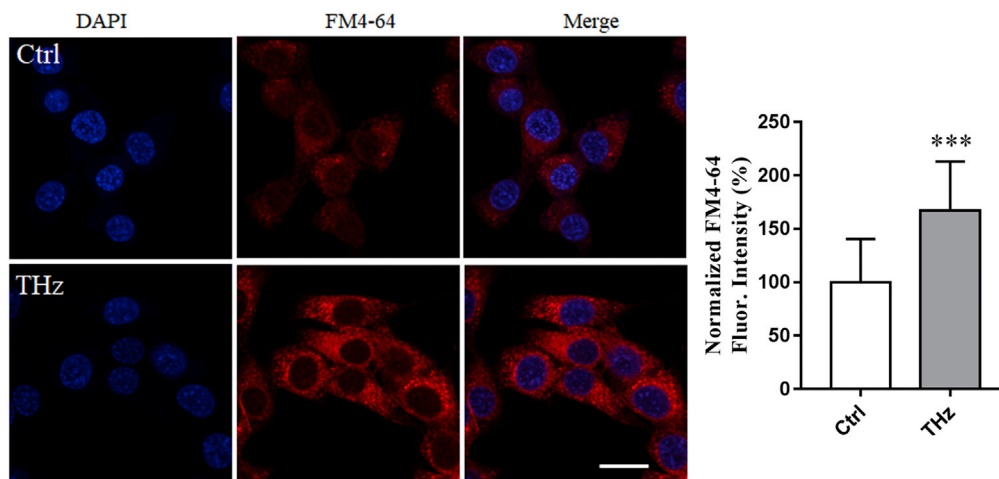


Figure 2. THz radiation enhanced endocytosis in neuronal cells

HT22 cells were stained with 10 μM FM4-64 and immediately exposed to 0.1 THz radiation at 33 mW/cm^2 for 5 min. The cells were then imaged using a laser scanning confocal microscope. Scale bar, 20 μm . The results are shown as Mean \pm SD. Statistical analyses were performed using two-tailed Student's *t* test (***p* < 0.001).

inhibited by Dynasore without THz irradiation. Interestingly, 0.1 THz irradiation still resulted in an increase of FM4-64 fluorescence signal in HT22 cells, indicating that 0.1 THz continuous wave irradiation could also promote the dynamin-independent endocytic process (Figure 3).

0.1 THz radiation facilitates the diffusion of rhodamine across the membrane

In addition to endocytosis, many small molecules also cross the cell membrane via passive diffusion (Yang and Hinner, 2015). We further investigated the effect of 0.1 THz radiation on the uptake of exogenous small molecules and explored whether 0.1 THz radiation may also affect the passive diffusion process. HT22 cells were incubated with a permeable fluorescent dye rhodamine B (RhB) under the treatment of 0.1 THz radiation. The amount of RhB inside the cells was analyzed using laser confocal microscopy and quantified by ImageJ after THz exposure. More RhB fluorescence signal was observed in the cells from the THz-irradiated group and quantitative analysis also indicated that the average fluorescence intensity of individual cells in the irradiated group was around 32% higher than that in the nonirradiated group (Figure 4A). In addition, the uptake of another rhodamine derivative, Rh123, was also tested in HT22 cells. As shown in Figure 4B, 0.1 THz radiation at 33 mW/cm^2 resulted in a significant increase of Rh123 fluorescence in the cytoplasm. Consistently, similar results were obtained in the PC12-based experiments following the identical procedures (Figure S3), which also confirmed that 0.1 THz radiation enhanced the uptake of exogenous small molecules.

Dynasore was also used to verify that the THz-induced enhancement of RhB uptake was mediated mainly by the diffusion process. As expected, Dynasore did not affect the uptake of RhB by HT22 cells. Meanwhile, it also could not diminish the 0.1 THz radiation-induced increase of RhB uptake in HT22 cells (Figure 5). These results showed that 0.1 THz radiation facilitated the RhB permeation in an endocytosis-independent manner which may be because of the increased cell membrane permeability resulting from THz exposure.

0.1 THz radiation facilitated the transport of GDC-0941 and H89 into cells

To further confirm the potential application of 0.1 THz continuous waves in facilitating small molecule permeation, another two hydrophobic chemical compounds were used to perform a biochemical experiment. GDC-0941 is an inhibitor of phosphoinositide 3-kinase (PI3K). Activation of PI3K in response to insulin stimulation results in the phosphorylation of its downstream effector, protein kinase B (PKB or Akt). When GDC-0941 enters the cells, it will inhibit the activity of PI3K and consequently results in the decrease of phosphorylated Akt level. Therefore, the level of phosphorylated Akt can be used to assess the amount of GDC-0941 entering the cell during a given period. HT22 cells were first incubated with 100 nM GDC-0941 for 10 min followed by 0.1 THz radiation for another 20 min. Then 1 μM insulin was used to stimulate the cells for 5 min. Total Akt and phosphorylated Akt (*p*-Akt) levels were detected by western blot analysis.

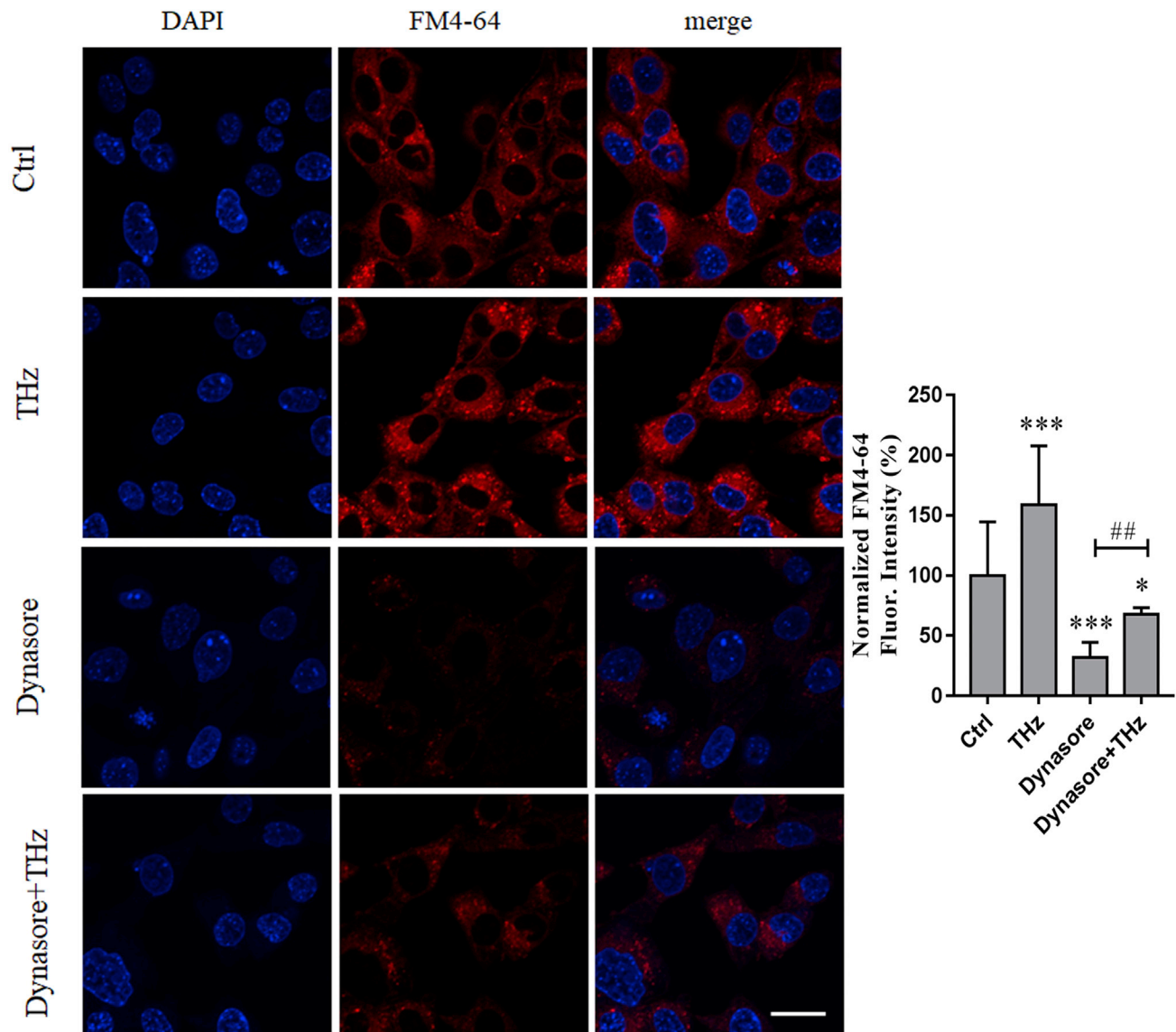


Figure 3. Irradiation-induced endocytosis was independent of dynamin

HT22 cells were treated with 10 μ M Dynasore or left untreated for 30 min, and subsequently stained with 10 μ M FM4-64 and immediately exposed to 0.1 THz irradiation at 33 mW/cm^2 for another 5 min. The cells were then imaged using a confocal laser scanning microscope. Scale bar, 20 μ m. The results are shown as means \pm SD. Statistical analyses were performed using ANOVA followed by Tukey's post hoc test (** $p < 0.01$, *** $p < 0.001$ vs. Ctrl group; ## $p < 0.01$ vs. Dynasore alone group).

As shown in Figure 6A, the p -AKT levels were significantly increased by insulin stimulation in HT22 cells and GDC-0941 attenuated the insulin-induced increase of p -AKT. At the same time, 0.1 THz radiation at an average power density of 33 mW/cm^2 triggered a further decrease of the p -AKT level. A similar trend was also observed in cells exposed to 7.8 mW/cm^2 THz irradiation although there was no statistical significance. In addition, THz radiation alone did not affect the p -AKT levels in the absence of GDC-0941 (Figure 6B). Therefore, it is reasonable to assume that more GDC-0941 entered the cells under the 0.1 THz irradiation, which resulted in a stronger inhibition of PI3K and a consequent lower level of p -AKT.

To test whether the change of membrane permeability upon 0.1 THz irradiation was only specific to GDC-0941, we repeated the same experiments with another hydrophobic small molecule, the protein kinase A (PKA) inhibitor H89. Here, the level of phosphorylated CREB (p -CREB) was chosen to assess the effect of

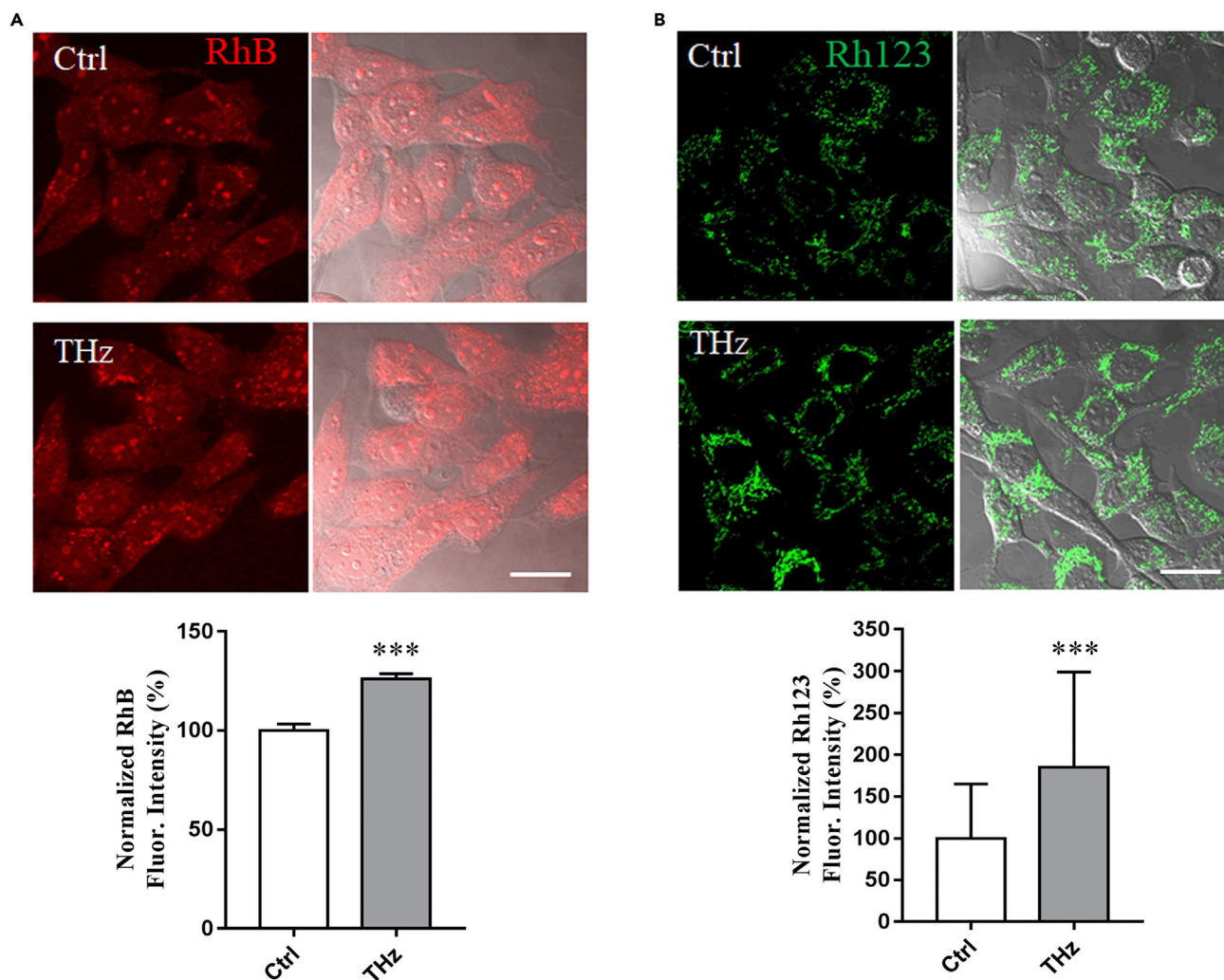


Figure 4. THz irradiation increased the diffusion of rhodamine into cells

(A) Exposure to THz irradiation increased the diffusion of rhodamine (Rh) B into the cells. HT22 cells were treated with 5 μM RhB and immediately exposed to 0.1 THz irradiation at 33 mW/cm^2 for 5 min. The cells were then imaged using a laser scanning confocal microscope.

(B) Exposure to THz irradiation increased the diffusion of the rhodamine derivative Rh123 into the cells. HT22 cells were treated with 5 μM Rh123 and immediately exposed to 0.1 THz irradiation at 33 mW/cm^2 for 5 min. The cells were then imaged using a confocal laser scanning microscope. Scale bar, 20 μm . The results are shown as means \pm SD. Statistical analyses were performed using two-tailed Student's *t* test (***p* < 0.001).

THz radiation on the membrane permeability of H89. PKA is an important kinase that directly phosphorylates CREB at Ser¹³³ (Naqvi et al., 2014). HT22 cells were treated with 10 μM H89 for 10 min followed by THz radiation for another 20 min. Then 10 μM forskolin was immediately added to activate the PKA/CREB signaling pathway. As expected, forskolin induced a significant increase in the *p*-CREB level, which was inhibited by H89. Furthermore, exposure to THz radiation significantly reduced the forskolin-induced increase of *p*-CREB (Figure 6C), which was consistent with the results obtained in the GDC-0941-based experiments. Notably, 0.1 THz radiation did not alter the basal level of *p*-CREB (Figure 6D), indicating that PKA activity was not disturbed by 0.1 THz radiation in the absence of H89 and forskolin and the further reduction of *p*-CREB in 0.1 THz exposed group was most likely because of the increase of H89 entering cells. Taken together, these results indicated that 0.1 THz radiation can increase the membrane permeability of HT22 cells and facilitate the transmembrane transport of small chemical compounds.

DISCUSSION

In this study, we uncovered a novel effect of low frequency THz continuous waves on the cell membrane permeability of neuronal cells. We found that 0.1 THz radiation promoted both the dynamin-dependent

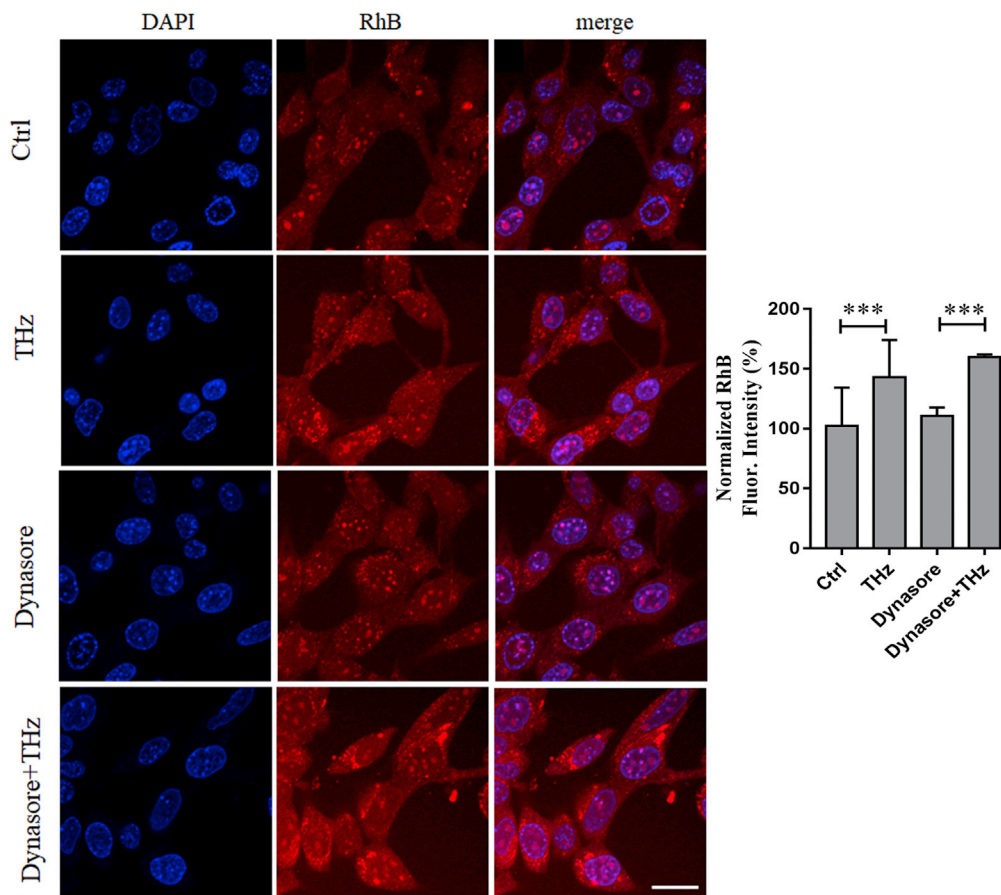


Figure 5. Irradiation-enhanced transport of RhB into the cells was not mediated by endocytosis

HT22 cells were treated with 10 μ M Dynasore or left untreated for 30 min, and subsequently stained with 5 μ M of RhB and immediately exposed to 0.1 THz irradiation at 33 mW/cm² for another 5 min. The cells were then imaged using a confocal laser scanning microscope. Scale bar, 20 μ m. The results are shown as means \pm SD. Statistical analyses were performed using two-tailed Student's *t* test (***p* < 0.001).

and the dynamin-independent endocytic process and facilitated the diffusion of small molecules across the plasma membrane of neuronal cells. This opens a new paradigm for understanding the biological effects of low frequency THz waves and hints at their potential application in regulating cell membrane functions.

Recently, we found that the endocytic activity of HT22 cells could be significantly altered by the 3.1 THz high-power pulses (Erling et al., 2022) as well as the 2.42 THz high-power pulses (data not shown). In this regard, THz irradiation for 5 min enhanced the FM4-64 labeled endocytosis of HT22 when cells were resting, and inhibited this process when cells were excited (Erling et al., 2022). In this study, we also found that cellular endocytosis could be promoted by 0.1 THz radiation, too. Endocytosis is a fundamental cellular function that mediates exogenous substance transport. It's not only involved in nutrient uptake, pathogen removal, and transporting signaling molecules from extracellular environment to intracellular cytoplasm (Conner and Schmid, 2003), but also plays an important role in cell signaling through the trafficking of membrane receptors (Benmerah and Lamaze, 2007). This process is usually accompanied by membrane invagination and budding of specialized domains of the plasma membrane, which involves complex mechanisms and numerous proteins (Wu et al., 2014). In addition to the frequencies we mentioned, Perera et al. also found that exposure to THz radiation at frequencies ranging from 0.3 to 19.5 THz promoted the endocytic activity of PC12 pheochromocytoma cells, in which irradiation for 10 min induced the formation of large blebs (up to 1 μ m) in the plasma membrane and triggered an increase of nanoparticle uptake (Perera et al., 2019). These studies indicated that several THz irradiations with different frequencies and waveforms affected cellular endocytosis, suggesting that the influence of THz radiation on plasma membrane endocytosis may not be limited to some specific frequencies. It also

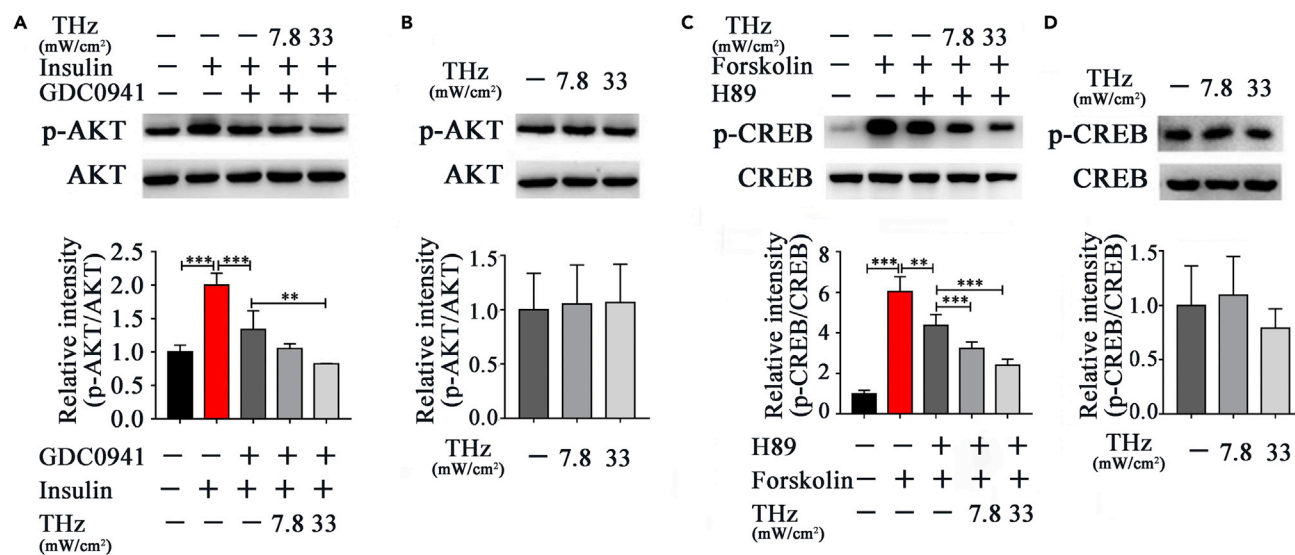


Figure 6. THz irradiation promoted the diffusion of the kinase inhibitors GDC0941 and H89 into neuronal cells

(A) Phosphorylated AKT (p-AKT) decreased upon THz exposure in the presence of GDC-0941. HT22 cells were treated with 100 nM GDC-0941 or left untreated for 10 min and subsequently exposed to 0.1 THz irradiation at 7.8 or 33 mW/cm² for another 20 min. Then, 1 μM of insulin was added to induce an increase in p-AKT level immediately after THz irradiation. P-AKT and AKT protein levels were analyzed by western blotting.

(B) THz irradiation did not affect p-AKT in the absence of GDC-0941. HT22 cells exposed to 0.1 THz irradiation at 7.8 or 33 mW/cm² for 20 min were analyzed by western blotting.

(C) Phosphorylated CREB (p-CREB) decreased upon THz exposure in the presence of H89. HT22 cells were treated with 10 μM H89 or left untreated for 10 min and subsequently exposed to 0.1 THz irradiation at 7.8 or 33 mW/cm² for another 20 min. Then 10 μM forskolin was added to induce an increase of the p-CREB level immediately after THz irradiation. p-CREB and CREB protein levels were analyzed by western blotting.

(D) THz irradiation did not affect p-CREB in the absence of H89. HT22 cells exposed to 0.1 THz irradiation at 7.8 or 33 mW/cm² for 20 min were analyzed by western blotting. The results are shown as means ± SD. Statistical analyses were performed using ANOVA followed by Tukey's post hoc test (**p < 0.01, ***p < 0.001).

implies that THz radiation might exert some more effects on cellular physiological processes via affecting endocytosis. It is quite interesting to find that the effect of 0.1 THz could not be totally blocked by the dynamin inhibitor, Dynasore. As an inhibitor of dynamin1, dynamin2, and Drp1, Dynasore inhibits the major dynamin-dependent endocytic process (Macia et al., 2006). Endocytosis labeled by FM4-64 was still enhanced by 0.1 THz radiation in the presence of Dynasore, suggesting that the dynamin-independent endocytic process might be activated upon 0.1 THz exposure. The dynamin-independent endocytic process is mainly regulated by Ca²⁺ and Rab5b (Jiang and Chen, 2009). Rab5b is a small GTPase which functions specifically in the formation and trafficking of early endosomes (Bucci et al., 1992). Our previous study demonstrated that 0.1 THz radiation did not induce any significant change of Ca²⁺ signal (data not shown), it did alter the gene expression of GTPase (Shang et al., 2021). Therefore, it is quite necessary and valuable to explore the effects of THz on GTPase activity and the detailed underlying biophysical mechanisms in the future.

Moreover, we revealed that the passive diffusion of small molecules could be enhanced by 0.1 THz radiation in this study. Two rhodamine derivatives, RhB and Rh123, which are membrane-permeable fluorescent dyes, were observed to accumulate more in the cytoplasm upon THz irradiation. Dynasore did not inhibit the uptake of RhB by cells, which confirmed that RhB mainly crossed the plasma membrane by diffusion (Johnson et al., 1980). The biochemical experiments carried out with the small compounds GDC-0941 and H89 provided additional evidence which also indicated that the cellular uptake of small molecules could be enhanced by 0.1 THz radiation. Although 33 mW/cm² THz irradiation resulted in a more significant reduction of p-AKT and p-CREB than 7.8 mW/cm² THz irradiation in this study, implying that the power density might be an influence factor that determines the effect of THz on the cell membrane. These results showed that the cell membrane properties and functions were extensively influenced by 0.1 THz radiation.

The cell membrane is a complex composite of multiple lipid species and proteins (Alberts, 2010). The interactions among these lipids and proteins may have been altered in response to THz wave exposure. It has

been reported that the protein-protein interactions could be affected by THz. Yamazaki and colleagues found that 0.46 THz radiation promoted the polymerization of actin *in vitro* (Yamazaki et al., 2018). However, they also observed the collapse of actin filaments in living cells after exposure to 80 $\mu\text{J}/\text{cm}^2$ THz micro-pulses for 30 min (Yamazaki et al., 2020). An earlier study showed that the interaction between antigen and antibody was reduced by 0.1 THz radiation at 80 mW/cm^2 (Homenko et al., 2009). These results suggest that THz radiation can modulate protein properties and interactions. In our previous work, we found that several phospholipids of the cell membrane such as DPPC, DSPE, and sphingomyelin, showed identical absorption peaks in the range of one–three THz (under submission). Although the frequency of the absorption peaks is different from that used in the present work, it still could be speculated that THz radiation was able to be absorbed by the membrane lipids as well as the protein components, subsequently affecting the lipid-lipid and lipid-protein interactions as well as the rearrangement of biomolecules in the cell membrane, potentially leading to the observed changes of cell membrane functions. Besides, molecular dynamic simulations of 1-palmitoyl-2-oleoyl-*sn*-glycero-3-phosphocholine (POPC) bilayers showed that THz radiation induced water intrusion and water bridge formation in the interior of membranes, accompanied by phospholipid redistribution into the water defect regions (Vernier et al., 2015), suggesting that THz-induced lipid electropores could change the membrane permeability for ion. Tang and colleagues reported the molecular dynamics simulation of the changes of water molecular dipole moment and total potential energy of the system and found that the electric field pulse train generated by 0.1–0.9 THz repetition frequency could cause phospholipid membrane perforation (Tang et al., 2020). Although the waveform we used might be not completely the same as Tang's, the simulation suggested that 0.1 THz-induced perforations of the membrane could facilitate the transmembrane transport of small molecules. More experiments and theoretical calculations need to be done to verify this effect in our future study. Moreover, 0.1 THz continuous wave could change the interaction between proteins (Homenko et al., 2009). Ramundo-Orlando et al. found that 0.13 THz could affect the interaction of phospholipids and the permeability of lipid bilayer (Ramundo-Orlando et al., 2007). Therefore, the intermolecular interactions of protein and/or phospholipids are likely affected by 0.1 THz in our study, which might further influence the membrane fluidity as well as the permeability. The combined effects of 0.1 THz radiation on cell membranes might result in the increased transmembrane transport of small molecules including RhB, Rh123, GDC0941, and H89. However, the comprehensive scientific evidence is yet to be revealed by more experiments and theoretical calculations in our future studies. In addition, THz radiation can be absorbed by water molecules. As a result, the strong dipole movements of the water molecules are affected and the temperature could increase (Perera et al., 2019). Although we speculated that the increased uptake of small molecules and the enhanced endocytic activity were because of the nonthermal effects of THz radiation because there was no detectable change in the temperature of the culture medium ($\pm 0.3^\circ\text{C}$) during the exposure, the local thermal variation and the molecular motion activities should be further investigated either by the experimental detection or the theoretical calculation. Besides, more experiments are also needed to further illustrate the relationships between various THz frequencies, power density, and the THz effects on cell membrane functions.

In summary, our results revealed that 0.1 THz radiation extensively affected the functions of the plasma membrane, facilitating the transmembrane transport of exogenous cargo. It opens up a broad space for studying the effects of THz on cellular materials exchange and information transmission. It also hints at the potential applications of THz radiation in biotechnology and biomedical fields in regulating cell membrane functions. Further studies defining the detailed mechanisms may help us to understand more basic and interesting interactions between THz waves and biomembrane systems.

Limitations of the study

The potential biophysical mechanism of 0.1 THz radiation on the cell membrane function needs further investigation.

STAR★METHODS

Detailed methods are provided in the online version of this paper and include the following:

- [KEY RESOURCES TABLE](#)
- [RESOURCE AVAILABILITY](#)
 - Lead contact
 - Materials availability

- Data and code availability
- EXPERIMENTAL MODEL AND SUBJECT DETAILS
- METHOD DETAILS
 - THz irradiation system
 - Cell treatment
 - Fluorescent images analysis
 - Western blot analysis
- QUANTIFICATION AND STATISTICAL ANALYSIS

SUPPLEMENTAL INFORMATION

Supplemental information can be found online at <https://doi.org/10.1016/j.isci.2022.103966>.

ACKNOWLEDGMENTS

We thank Dr. Changhe Wang of Xi'an Jiaotong University for his kind suggestions to our work. We also thank Mrs. Ying Hao at the Instrumental Analysis Center of Xi'an Jiaotong University for her technical assistance. This work was supported by the National Natural Science Foundation of China and China Academy of Engineering Physics (J2030105).

AUTHOR CONTRIBUTIONS

X. L. conceived the project. X. L. and E. H. designed the experiments. E. H., Q. Z., S. S., and Y. J. performed the experiments, as well as analyzed and interpreted the data. X. L., E. H., and Q. Z. drafted the manuscript. All authors approved the final version of the manuscript. X. L. is the guarantor of this work and takes responsibility for the integrity of the data and the accuracy of the data analysis.

DECLARATION OF INTERESTS

The authors declare no competing interests.

Received: September 15, 2021

Revised: January 19, 2022

Accepted: February 18, 2022

Published: March 18, 2022

REFERENCES

- Abufadda, M.H., Erdelyi, A., Pollak, E., Nugraha, P.S., Hebling, J., Fulop, J.A., and Molnar, L. (2021). Terahertz pulses induce segment renewal via cell proliferation and differentiation overriding the endogenous regeneration program of the earthworm *Eisenia andrei*. *Biomed. Opt. Express* 12, 1947–1961.
- Alberts, B. (2010). Cell biology: the endless frontier. *Mol. Biol. Cell* 21, 3785.
- Alexandrov, B.S., Rasmussen, K.O., Bishop, A.R., Usheva, A., Alexandrov, L.B., Chong, S., Dagon, Y., Booshehri, L.G., Mielke, C.H., Phipps, M.L., et al. (2011). Non-thermal effects of terahertz radiation on gene expression in mouse stem cells. *Biomed. Opt. Express* 2, 2679–2689.
- Baryawno, N., Sveinbjornsson, B., Eksborg, S., Chen, C.S., Kogner, P., and Johnsen, J.I. (2010). Small-molecule inhibitors of phosphatidylinositol 3-kinase/Akt signaling inhibit Wnt/beta-catenin pathway cross-talk and suppress medulloblastoma growth. *Cancer Res.* 70, 266–276.
- Benmerah, A., and Lamaze, C. (2007). Clathrin-coated pits: vive la difference? *Traffic* 8, 970–982.
- Borovkova, M., Khodzitsky, M., Demchenko, P., Cherkasova, O., Popov, A., and Meglinski, I. (2018). Terahertz time-domain spectroscopy for non-invasive assessment of water content in biological samples. *Biomed. Opt. Express* 9, 2266–2276.
- Bucci, C., Parton, R.G., Mather, I.H., Stunnenberg, H., Simons, K., Hoflack, B., and Zerial, M. (1992). The small GTPase rab5 functions as a regulatory factor in the early endocytic pathway. *Cell* 70, 715–728.
- Chen, S., Song, Z., and Zhang, A. (2019). Small-molecule immuno-oncology therapy: advances, challenges and new directions. *Curr. Top Med. Chem.* 19, 180–185.
- Cheng, Y., Wang, Y., Niu, Y., and Zhao, Z. (2020). Concealed object enhancement using multi-polarization information for passive millimeter and terahertz wave security screening. *Opt. Express* 28, 6350–6366.
- Cho, I.J., Woo, N.R., Shin, I.C., and Kim, S.G. (2009). H89, an inhibitor of PKA and MSK, inhibits cyclic-AMP response element binding protein-mediated MAPK phosphatase-1 induction by lipopolysaccharide. *Inflamm. Res.* 58, 863–872.
- Conner, S.D., and Schmid, S.L. (2003). Regulated portals of entry into the cell. *Nature* 422, 37–44.
- Elayan, H., Stefanini, C., Shubair, R.M., and Jornet, J.M. (2018). End-to-end noise model for intra-body terahertz nanoscale communication. *IEEE Trans. Nanobiosci.* 17, 464–473.
- Erling, H., Leilei, W., Qi, Z., Peng, L., Peng, Z., Dai, W., and Xiaoyun, L. (2022). Studying the influence of 3.1 THz irradiation on the endocytosis of neuronal cells. *J. Opt. Soc. Am. B* 39, 129–136.
- Ferguson, S.M., and De Camilli, P. (2012). Dynamin, a membrane-remodelling GTPase. *Nat. Rev. Mol. Cell Biol.* 13, 75–88.
- Ghann, W., Kang, H., Rahman, A.K., Rahman, A., Ali, M.M., and Uddin, J. (2019). Terahertz reflectometry imaging of carbon nanomaterials for biological application. *J. Nanomed. Nanotechnol.* 10, 535.
- Homenko, A., Kapilevich, B., Kornstein, R., and Firer, M.A. (2009). Effects of 100 GHz radiation on alkaline phosphatase activity and antigen-antibody interaction. *Bioelectromagnetics* 30, 167–175.

Jiang, M., and Chen, G. (2009). Ca²⁺ regulation of dynamin-independent endocytosis in cortical astrocytes. *J. Neurosci.* 29, 8063–8074.

Johnson, L.V., Walsh, M.L., and Chen, L.B. (1980). Localization of mitochondria in living cells with rhodamine 123. *Proc. Natl. Acad. Sci. U S A.* 77, 990–994.

Macia, E., Ehrlich, M., Massol, R., Boucrot, E., Brunner, C., and Kirchhausen, T. (2006). Dynasore, a cell-permeable inhibitor of dynamin. *Dev. Cell* 10, 839–850.

Naqvi, S., Martin, K.J., and Arthur, J.S. (2014). CREB phosphorylation at Ser133 regulates transcription via distinct mechanisms downstream of cAMP and MAPK signalling. *Biochem. J.* 458, 469–479.

Perera, P.G.T., Appadoo, D.R.T., Cheeseman, S., Wandiyanto, J.V., Linklater, D., Dekiwadia, C., Truong, V.K., Tobin, M.J., Vongsivut, J., Bazaka, O., et al. (2019). PC 12 pheochromocytoma cell response to super high frequency terahertz radiation from synchrotron source. *Cancers (Basel)* 11, 162.

Ramundo-Orlando, A., Gallerano, G.P., Stano, P., Doria, A., Giovenale, E., Messina, G., Cappelli, M., D'Arienzo, M., and Spassovsky, I. (2007). Permeability changes induced by 130 GHz pulsed

radiation on cationic liposomes loaded with carbonic anhydrase. *Bioelectromagnetics* 28, 587–598.

Romanenko, S., Begley, R., Harvey, A.R., Hool, L., and Wallace, V.P. (2017). The interaction between electromagnetic fields at megahertz, gigahertz and terahertz frequencies with cells, tissues and organisms: risks and potential. *J. R. Soc. Interf.* 14, 20170585.

Shang, S., Wu, X., Zhang, Q., Zhao, J., Hu, E., Wang, L., and Lu, X. (2021). 0.1 THz exposure affects primary hippocampus neuron gene expression via alternating transcription factor binding. *Biomed. Opt. Express* 12, 3729–3742.

Specht, E.A., Braselmann, E., and Palmer, A.E. (2017). A critical and comparative review of fluorescent tools for live-cell imaging. *Annu. Rev. Physiol.* 79, 93–117.

Tang, J., Ma, J., Guo, L., Wang, K., Yang, Y., Bo, W., Yang, L., Jiang, H., Wu, Z., Zeng, B., et al. (2020). The effect of KcsA channel on lipid bilayer electroporation induced by picosecond pulse trains. *J. Membr. Biol.* 253, 271–286.

Vernier, P.T., Levine, Z.A., Ho, M.C., Xiao, S., Semenov, I., and Pakhomov, A.G. (2015). Picosecond and terahertz perturbation of interfacial water and electropermeabilization of

biological membranes. *J. Membr. Biol.* 248, 837–847.

Williams, R., Schofield, A., Holder, G., Downes, J., Edgar, D., Harrison, P., Siggel-King, M., Surman, M., Dunning, D., Hill, S., et al. (2013). The influence of high intensity terahertz radiation on mammalian cell adhesion, proliferation and differentiation. *Phys. Med. Biol.* 58, 373–391.

Wu, L.G., Hamid, E., Shin, W., and Chiang, H.C. (2014). Exocytosis and endocytosis: modes, functions, and coupling mechanisms. *Annu. Rev. Physiol.* 76, 301–331.

Yamazaki, S., Harata, M., Idehara, T., Konagaya, K., Yokoyama, G., Hoshina, H., and Ogawa, Y. (2018). Actin polymerization is activated by terahertz irradiation. *Sci. Rep.* 8, 9990.

Yamazaki, S., Harata, M., Ueno, Y., Tsubouchi, M., Konagaya, K., Ogawa, Y., Isoyama, G., Otani, C., and Hoshina, H. (2020). Propagation of THz irradiation energy through aqueous layers: demolition of actin filaments in living cells. *Sci. Rep.* 10, 9008.

Yang, N.J., and Hinner, M.J. (2015). Getting across the cell membrane: an overview for small molecules, peptides, and proteins. *Methods Mol. Biol.* 1266, 29–53.

STAR★METHODS

KEY RESOURCES TABLE

REAGENT or RESOURCE	SOURCE	IDENTIFIER
Antibodies		
Mouse Anti-phospho-AKT	Proteintech, USA	66444-1-IG
Rabbit Anti-AKT	Proteintech, USA	10176-2-AP
Rabbit Anti-phospho-CREB	Cell Signaling Technology, USA	9198s
Rabbit Anti-CREB	Cell Signaling Technology, USA	9197s
HRP, Goat Anti-Rabbit IgG	Absin, China	abs-200002ss
HRP, Goat Anti-Mouse IgG	Absin, China/	abs-200001ss
Chemicals, peptides, and recombinant proteins		
Insulin	Beyotime, China	P3376
Forsklin	Beyotime, China	S1612
GDC0941	Topscience, China	T1994
H89	Beyotime, China	S1643
Dynasore	Topscience, China	T1848
Rhodamine B	Sigma, USA	81889
Rhodamine 123	Beyotime, China	C2007
FM4-64	Thermo Fisher, USA	T13320
DAPI	Thermo Fisher, USA	D3571
HRP Substrate	Millipore, USA	WBLUF0100
Mounting medium	Solarbio Life Science, China	S2100
4% paraformaldehyde	Biosharp, China	BL539A
Hank's balanced salt solution	Hyclone, USA	SH30030.02
SDS-PAGE Loading buffer	Beyotime, China	P0015
Bovine serum albumin	Sigma, USA	SRE0096
Experimental models: Cell lines		
PC12 pheochromocytoma cells	ATCC	CRL-1721
HT22 hippocampal neurons	Shanghai Honsun Biological Technology Company, China	N/A
Software and algorithms		
GraphPad Prism 7.0	GraphPad Software	https://www.graphpad.com/
FluorChem FC2 System	Alpha Innotech, USA	https://www.alphainnotech.com
ImageJ	ImageJ	https://imagej.nih.gov/ij/index.html
Other		
14 mm glass coverslips	NEST, China	801010
PVDF membranes	Millipore, USA	IPVH00010
infrared thermometer	ZyTemp, China	TN-40ALC
Confocal laser scanning microscope	Zeiss, Germany	LSM700

RESOURCE AVAILABILITY

Lead contact

Further information and requests for resources and reagents should be directed to and will be fulfilled by the lead contact, Xiaoyun Lu (luxy05@xjtu.edu.cn).

Materials availability

This study did not generate new unique reagents.

Data and code availability

- Data: Data reported in this paper will be shared by the lead contact upon request.
- Code: This paper does not report original codes.
- All other items: Any additional information required to reanalyze the data in this paper is available from the lead contact upon request.

EXPERIMENTAL MODEL AND SUBJECT DETAILS

This work did not need any unique experimental model.

METHOD DETAILS

THz irradiation system

In order to irradiate cell cultures with THz radiation, the terahertz source operating in 0.1 THz frequency purchased from the company of TeraSense (USA) was used. The terahertz source is developed based on the impact ionization Avalanche Transit-Time (IMPATT) diode, which is represented by silicon double drift diodes with a 0.6 μm transit region, mounted on a copper heat sink. The device relies on negative resistance to generate and sustain an oscillation, with the highest output power of 80 mW. The frequency line-width is smaller than 1 MHz. The modulator is transistor-transistor logic (TTL) modulation option with 1 μs rise/fall time. The experimental setup is shown in [Figure 1](#). The output THz wave was transported to a conical horn antenna rigidly attached at the bottom surface of the transparent plastic cell culture plate to irradiate the samples. Because water vapor attenuates most of the terahertz energy, the experiments were set up to minimize the space traveled by the radiation within the thermostat. The bottom of the thermostat can be heated and has a hole of 1.6 cm in diameter to allow radiation to pass through, the four walls are double vacuum Plexiglas to reduce heat loss. The thermostat was preheated before the radiation experiments to ensure that the temperature inside the thermostat was 37°C. The average power density of the irradiation received by the samples was either 33 or 7.8 mW/cm^2 , as indicated.

Cell treatment

Murine hippocampal neuronal cell line HT22 was cultured in 24-well flat-bottom plates with glass coverslips and incubated at 37°C in an atmosphere comprising 5% CO_2 overnight prior to assays with the fluorescent small molecules, rhodamine 123 or rhodamine B and FM4-64. In the irradiation experiment, the glass slide was turned over to ensure the cells were facing down and placed onto Hank's balanced salt solution containing 100 μL working solution of rhodamine or FM4-64. The cells were exposed to 0.1 THz waves in dye solution for 5 min, after which the dye solution was discarded and the cells washed with HBSS. Then, 4% paraformaldehyde was added and incubated for 15 min at room temperature. The fixed cells were stained with 5 $\mu\text{g}/\text{mL}$ of DAPI for 10 min or left unstained and washed with HBSS 3 times. Finally, the cells were mounted using anti-fading mounting medium and imaged using a confocal laser scanning microscope.

HT22 cells were seeded into 24-well flat-bottom plates for the assays with the small-molecule kinase inhibitors GDC-0941 and H89. In the irradiation experiment, the cells were pretreated with or without GDC-0941 or H89 for 10 min, after which the experimental group was exposed to THz radiation for 20 min. When the radiation was finished, 1 μM insulin or 10 μM forskolin was immediately added into the medium, respectively, and incubated with cells for another 5 min. Cells were then collected and cell lysate was applied to the western blot analysis.

Cells in all groups were kept at the same ambient temperature of 37°C throughout the irradiation process. The temperatures of the medium in each cell culture hole were measured by a hand-held infrared thermometer. For each experiment, at least 3 cell samples were used to perform the corresponding treatment and analysis.

Fluorescent images analysis

Fluorescent images got from confocal laser scanning microscopy were analyzed using the free NIH software ImageJ. At least 3 slides were prepared for each sample, and 3 fields for each slide were selected randomly to obtain images for analysis. In the fluorescence intensity analysis, the fluorescent images were firstly changed into a type of 8-bit image, and the Integrated Optica Density (IOD) each cell delineated by the threshold boundary was considered to be the average fluorescence density of each cell.



Western blot analysis

Samples were washed with PBS and then lysed with 1×loading buffer. Proteins were separated via SDS/PAGE and electro-blotted onto PVDF membranes. The protein-loaded PVDF-membranes were blocked with 5% bovine serum albumin for 1 h at room temperature and subsequently incubated with primary antibodies (anti-phospho-CREB, anti-CREB, anti-phospho-AKT, and anti-AKT) at 4°C overnight. The membranes were washed with TBST 3 times, followed by incubation with the horseradish peroxidase (HRP)-conjugated secondary antibodies for 1 h at room temperature, and subsequently washed with TBST 3 times before imaging. Protein bands were visualized using the FlorChem FC2 System with the Immobilon™ Western Chemiluminescent HRP Substrate.

QUANTIFICATION AND STATISTICAL ANALYSIS

Multi-group comparisons were performed using ANOVA followed by Tukey's post-hoc test. Comparisons between two groups were performed using Student's *t*-test. Differences with $p < 0.05$ were considered statistically significant. Error bars indicate the standard deviation (SD).